One-dimensional actuation of a ferrofluid droplet by planar microcoils

Ali Beyzavi, Nam-Trung Nguyen§

† School of Mechanical and Aerospace Engineering, Nanyang Technological University, 50 Nanyang Avenue, Singapore 639798

Abstract.

This paper discusses the simulation of a device for actuation of a ferrofluid droplet using planar microcoils. The device with two pairs of planar microcoils was designed and fabricated on a double-sided printed circuit board (PCB). Each pair is placed on one side of the PCB. The coils on the bottom actuate the droplet along the line connecting their centers. The coils on the top create a virtual channel to confine the motion of the droplet along a straight line. The paper first formulates the model of the magnetic field of the coils. With the modeled magnetic field, the corresponding forces acting on the droplet were calculated. The equation of the motion of a ferrofluid droplet immersed in silicon oil was solved numerically. The influence of different parameters such as driving current, droplet diameter and viscosity of the carrier fluid was investigated. Both theoretical and experimental results showed that a higher magnetic field, a lower oil viscosity and a bigger droplet size will increase the peak velocity of the droplet.

§ To whom correspondence should be addressed (mntnguyen@ntu.edu.sg)

1. Introduction

The field of microfluidics was originally established based on continuous flows, but later also branched towards using droplets [1, 2]. Droplet-based microfluidic systems pose many benefits such as reducing the time of chemical reactions, using smaller amount of samples, the possibility of using non-mechanical actuation concepts and the resulting increased reliability of the devices [3].

During the past decade, a few actuation concepts have been used to manipulate droplets. Electrostatic forces [4, 5], thermocapillarity [6], acoustics [7] and magnetism [8] are some of the examples. Compared to these concepts, magnetism for manipulation of droplets has certain advantages. Objects can be manipulated by an external magnetic field that is not in contact with the fluid. Furthermore, the effect of magnetic field on particles is generally not affected by surface charges, pH level, ionic concentration or temperature [8].

Ahn et al. used integrated inductive components for separation of magnetic micro beads [9]. Ramadan et al. discussed the use of current carrying wires for manipulating magnetic particles [10]. Lee et al. used a matrix of microcoils and a ring trap to position and control magnetic micro/nanoparticles [11]. Rida et al. transported magnetic beads in a glass capillary for a long range using planar coils [12]. Lehmann et al. manipulated magnetic beads suspended in a droplet by planar microcoils [13]. Lee et al. fabricated a device with integrated microcoils for manipulating cells tagged by magnetic beads [14].

Magnetic beads have diameters ranging from 250 nm to 6 μm, while ferrofluid has particles on the order of a few nanometers [15]. The larger size of magnetic beads causes redistribution of the beads in a droplet. In the worst case, the droplet may be split into two parts, one with and the other without magnetic beads. The one without the beads can no longer be manipulated by the magnetic force. In a ferrofluid droplet, magnetic particles have sizes on the order of nanometers, thus the random motion of the particles overcomes the magnetic force and the homogenous distribution of the particles in the droplet is not affected by the magnetic field. Therefore, compared to droplets containing magnetic beads ferrofluid droplets are a more suitable candidate for magnetic actuation. Guo et al. demonstrated the manipulation of water-based ferrofluid droplets on a hydrophobic surface using permanent magnets [16]. Nguyen et al. manipulated ferrofluid droplets immersed in silicon oil using planar microcoils [17]. His research group also used a magnetically driven ferrofluid plug for a polymerase chain reaction (PCR) device [18]. In this paper, the actuation mechanism of magnetic manipulation using planar coils is modeled in details. Mathematical models for both magnetic field and the droplet motion are formulated and solved. Theoretical results are then compared with the experimental results reported earlier in [17]

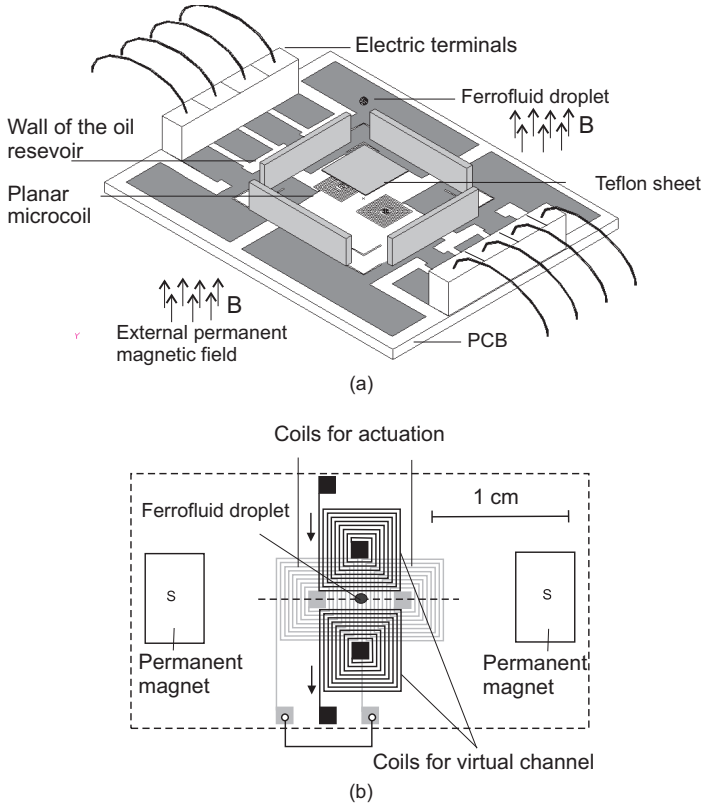

Figure 1. The PCB device for manipulation of a ferrofluid droplet: (a) The 3-D view of the device; (b) The device components [15].

2. Modeling of the magnetic field

In a magnetic field, magnetic particles are attracted to the field maximum [19]. The manipulation of the droplet in our device is based on changing the location of magnetic field maximum. Switching the peak of the magnetic field can move the droplet back and forth. Figure 1 shows the device used in our analysis and experiments. The device has two pairs of planar microcoils. Each pair is located on each side of a double-sided printed circuit board (PCB). A reservoir is made around the coils on the top side to contain silicon oil as carrier fluid. A ferrofluid droplet is placed on a Teflon sheet inside the reservoir. The ferrofluid droplet is immersed in silicon oil and actuated by the magnetic field of the planar microcoils. The magnetic field of the top coils creates a virtual channel to limit the droplet motion along the x-axis, while the bottom coils provide the actuation force. The following section reports the model of the magnetic field induced by two planar coils.

2.1. Modeling the magnetic field of a pair of planar microcoils

The planar microcoils depicted in Fig. 1 consist of a series of wire segments with a finite length [Figure 2 (a)]. The magnetic field of a wire segment with finite length can

be obtained by solving the Biot and Savart's integral [20]. Superimposing the magnetic field of the wire segments results in all components of the magnetic field of a single planar microcoil [21]:

$$H_{x,\text{coil}} = \sum_{i=1}^{n} H_{x,i},\ H_{y,\text{coil}} = \sum_{i=1}^{n} H_{y,i},\ H_{z,\text{coil}} = \sum_{i=1}^{n} H_{z,i}, \tag{1}$$

where n is the the total number of segments in a coil and $H_{x,i}$, $H_{y,i}$, $H_{z,i}$ are the x, y and z components of wires in a single planar microcoil respectively. Superimposing the magnetic field of two coils results in the combined magnetic field:

$$\begin{aligned} H_x &= H_{x,\text{coil1}} + H_{x,\text{coil2}} \\ H_y &= H_{y,\text{coil1}} + H_{y,\text{coil2}} \\ H_z &= H_{z,\text{coil1}} + H_{z,\text{coil2}} \end{aligned} \tag{2}$$

The total magnitude of the field strength is then:

$$H_{\text{total}} = \sqrt{H_x^2 + H_y^2 + H_z^2} \tag{3}$$

The magnetic flux $\mathbf{B}$ can subsequently be obtained by:

$$\mathbf{B} = \mu_0 \mathbf{H}(1 + \chi_{\text{m}}) \tag{4}$$

where χ_{m} is the magnetic susceptibility of the medium in which the magnetic field is to be calculated and $\mu_0 = 4\pi \times 10^{-7}$ is the permeability of free space.

The magnetic field on the line connecting the centers of two coils was measured using a Gauss meter (GM05, Hirst magnetic instrument, UK), in order to validate the model for the two coils. The theoretical model was implemented and calculated in Matlab (MathWorks Inc, USA). The distribution of the field strength was determined for a line running along the x-axis and through the center of the two coils. Figure 3 shows that the experimental and theoretical results of the magnetic field agree relatively well.

2.2. Actuation Mechanism

The above model of the magnetic field can be used to describe the actuation mechanism for the device depicted in Fig. 1. As mentioned above, the two coils on the back side of the PCB are used to move the droplet. Without a permanent magnetic field, there are two field maxima at the two coil centers where the ferrofluid will be trapped, Fig. 2. Thus, actuation will not be possible without the superposition of an external permanent magnetic field. If the currents in these two coils are running in opposite directions, the superposition with the external permanent magnetic field creates a single peak of the total magnetic field strength H_{total} as shown in Figure 4. A pair of permanent magnets create a homogenous magnetic field in the area between the two coils, Figure 1 (b). The ferrofluid droplet is attracted by this single field maximum. The field of the permanent magnets also helps to increase the magnetic force acting on the ferrofluid droplet. If the currents in the two coils reverse their direction, the location of the field maximum also shifts from the center of one coil to the center of the other coil. Using an electronic

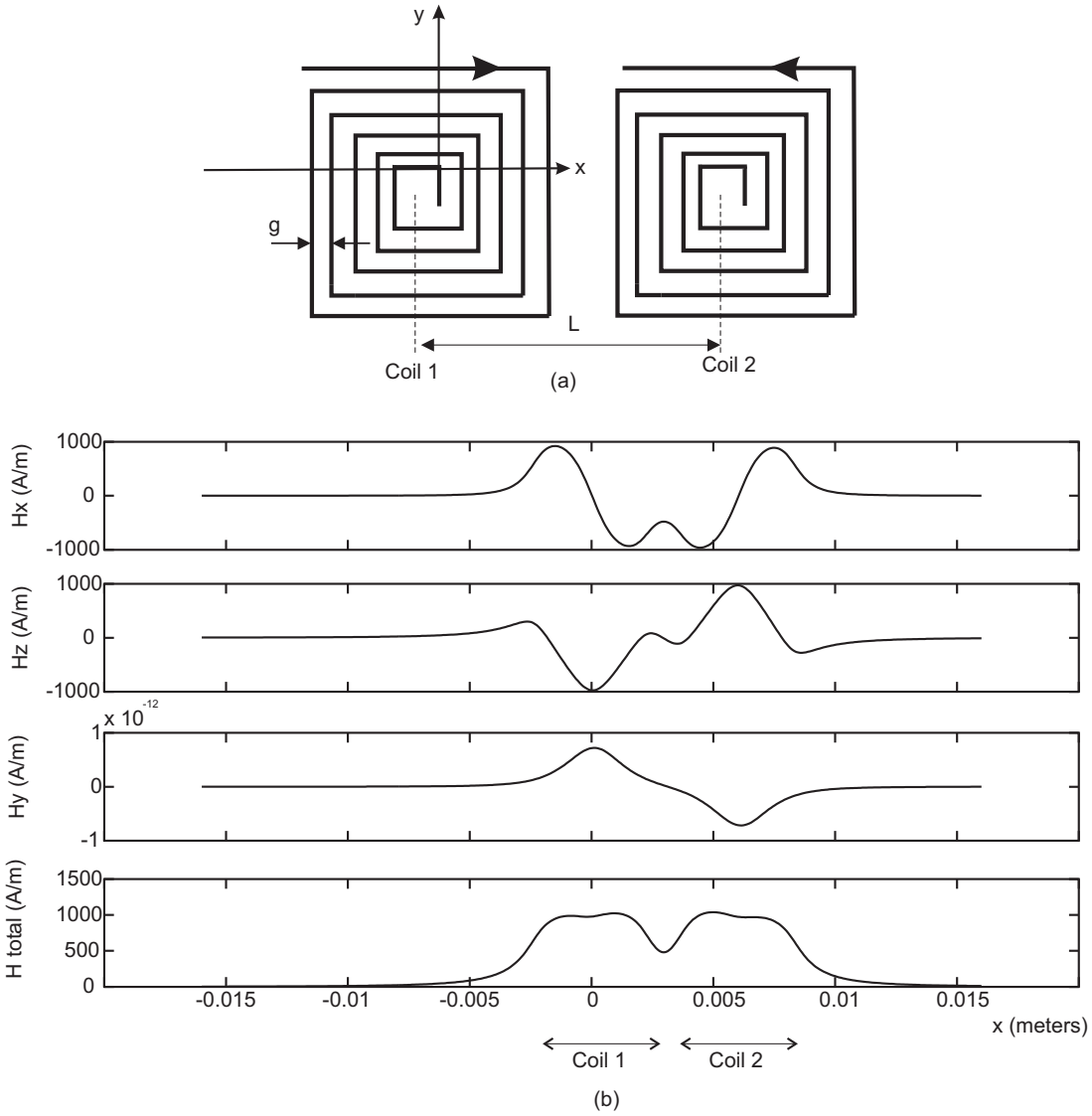

Figure 2. The magnetic field of the driving coils at $y = 0$ mm, $z = 0.75$ mm (without superposition with external permanent field, coils have opposite polarities, number of segments n=47, current I=0.8 A, gap between segments $g = 200$ μm), center-to-center distance $L = 6$ mm): (a) Arrangement of the coils and the coordinate; (b) Three components of the magnetic field strength.

control circuit and the experimental setup reported previously [17], the location of the field maximum can be switched periodically causing the ferrofluid droplet to move back and forth along the x axis.

The two coils on the top of the PCB as depicted in Figure 1(a) are used to make a virtual channel to confine the droplet along the x-axis. In this case, the field maximum should be located between the two coils. Figure 5 shows the simulation results of two coils with the same field polarity and the same magnitude. After adding the homogenous field of the permanent magnets, only a single peak of the field strength is located between them. This field maximum acts as a trap and keeps the ferrofluid droplet on the line

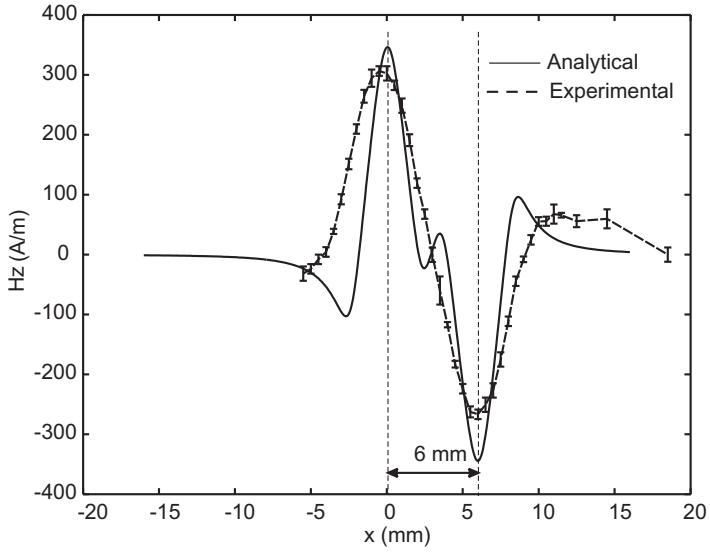

Figure 3. The z-component of the magnetic field strength (I=0.3A, n=47, center-to-center distance $L = 6$ mm, measured position $y = 0$ mm and $z = 0.8$ mm).

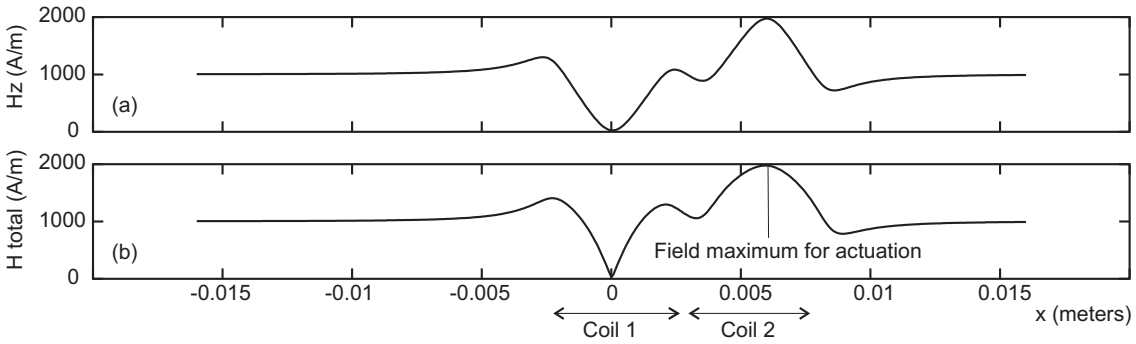

Figure 4. The magnetic field of the driving coils at $y = 0$ mm, $z = 0.75$ mm (with superposition with external permanent field in z-axis, coils have opposite polarities, number of segments n=47, current I=0.8 A, gap between segments $g = 50$ μm, center-to-center distance $L = 6$ mm, permanent field strength $H_0 = 1000$ A/m): (a) z component of the resultant magnetic field; (b) The total magnetic field.

connecting the centers of the actuating coils on the other side of the PCB.

3. Modeling of magnetic actuation of a ferrofluid droplet

3.1. Forces acting on the droplet moving in silicon oil

With the device depicted in Figure 1, the ferrofluid droplet is immersed in oil and actuated by the magnetic force. The kinematic behavior of the droplet is determined by the forces acting on it. The ferrofluid droplet is assumed to have a spherical shape. This assumption is justified based on the measurement of the contact angle between the ferrofluid and the Teflon sheet. The contact angle of a ferrofluid droplet and the Teflon

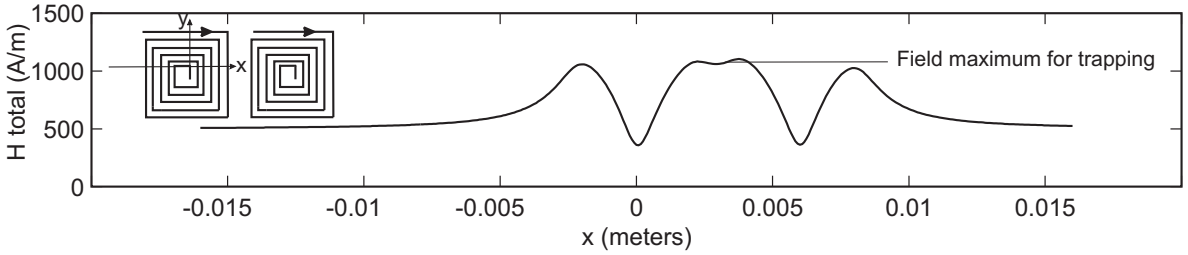

Figure 5. The magnetic field of the coils for virtual channel at $y = 0$ mm, $z = 1$ mm (with superposition with external permanent field in z-axis $H_0 = 500$ A/m, coils have the same polarity, number of segments n=47, current I=0.8 A, gap between segments $g = 200$ μm, center-to-center distance $L = 6$ mm)

surface immersed in silicone oil was measured as 127° using a tensiometer (FTA200, First Ten Angstrom) [17].

The inertial force, the drag force and the driving magnetic force are three forces acting on the ferrofluid droplet when it moves in silicon oil. Considering the assumption of spherical droplet, the drag force is calculated as [22]:

$$F_{\text{drag}} = 3\pi D\eta U \frac{1 - 2\eta/3\eta_{ff}}{1 + \eta/\eta_{ff}} \tag{5}$$

where D is the diameter of the droplet, η is the dynamic viscosity of the carrier fluid (silicon oil), η_{ff} is the dynamic viscosity of the ferrofluid and U is the velocity of the droplet in oil. If the viscosity of the ferrofluid is much larger than that of the silicone oil $\eta_{ff} >> \eta$, the drag force can be simplified as:

$$F_{\text{drag}} = 3\pi D\eta U \tag{6}$$

In a system with two coils, the magnetic force can be calculated by superposition of the magnetic forces of both coils. The magnetic force acting on the ferrofluid droplet with a volume V is

$$\mathbf{F} = \frac{V\Delta\chi}{\mu_0}(\mathbf{B}.\nabla)\mathbf{B} \tag{7}$$

and can be formulated in the three spacial components as:

$$\begin{aligned} F_x &= \tfrac{V\Delta\chi}{\mu_0}(B_x\tfrac{\partial B_x}{\partial x} + B_y\tfrac{\partial B_x}{\partial y} + B_z\tfrac{\partial B_x}{\partial z}) \\ F_y &= \tfrac{V\Delta\chi}{\mu_0}(B_x\tfrac{\partial B_y}{\partial x} + B_y\tfrac{\partial B_y}{\partial y} + B_z\tfrac{\partial B_y}{\partial z}) \\ F_z &= \tfrac{V\Delta\chi}{\mu_0}(B_x\tfrac{\partial B_z}{\partial x} + B_y\tfrac{\partial B_z}{\partial y} + B_z\tfrac{\partial B_z}{\partial z}) \end{aligned} \quad . \tag{8}$$

The resultant magnetic force of two coils is determined by superposition:

$$\begin{aligned} F_{x,\text{total}} &= F_{x,\text{coil1}} + F_{x,\text{coil2}} \\ F_{y,\text{total}} &= F_{y,\text{coil1}} + F_{y,\text{coil2}} \\ F_{z,\text{total}} &= F_{z,\text{coil1}} + F_{z,\text{coil2}} \end{aligned} \tag{9}$$

Since the droplet is actuated one-dimensionally along the x axis and its motion in other directions is confined by the virtual channel, only the force component F_x is considered in our subsequent model. The magnetic field of the permanent magnets is also

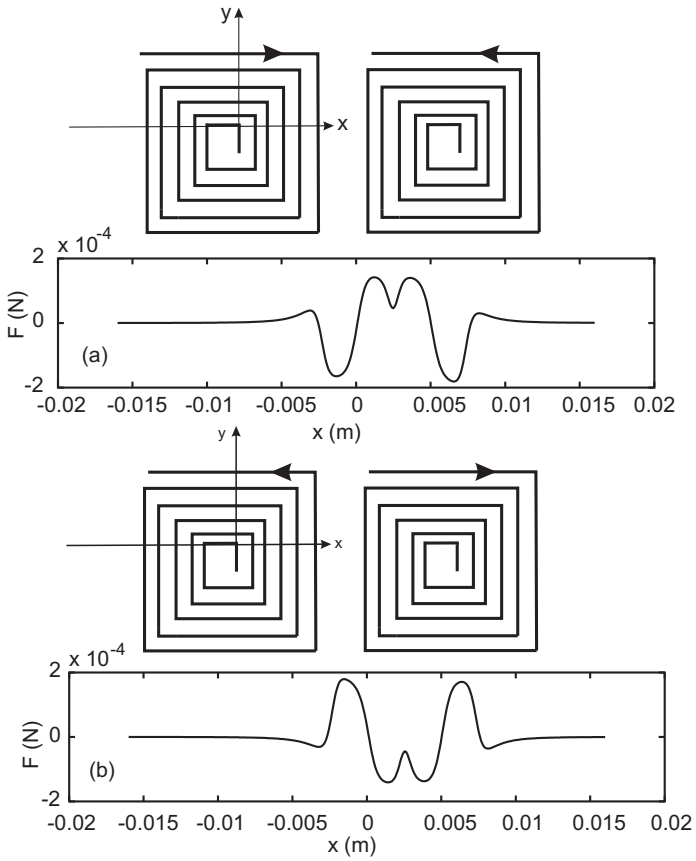

Figure 6. The direction of the force between two coils acting on the droplet changes by changing the current direction (y = 0 mm, z = 1 mm , driving current I=0.7 A, number of segments n=47, gap between segments g = 200 μm, center-to-center distance L = 6 mm, permanent field strength H_0 = 1000 A/m).

considered. Measurements showed that the magnetic field strength H_0 of the permanent magnets used in our experiments ranges from 500 to 8000 A/m in the actuation domain, depending on their positions. Figure 6 shows the modeled magnetic force distribution for a ferrofluid droplet with a diameter of 1mm. The results show that the force acting on the droplet changes its sign or direction, if the direction of the current is reversed.

The center-to-center distance between two coils affects the force distribution. Figure 7 depicts the simulated force distribution for different center-to-center distances. If the coils are close enough, the droplet will experience the maximum force between the two coil centers, Fig. 7(a). At an optimum distance, an almost constant magnetic force can be achieved, Fig. 7(b). In order to actuate the droplet between the two coil centers, the force between the two coil centers should not change its sign. If the coils are placed too far apart, the magnetic force may change its direction making actuation between the coil centers impossible, Fig. 7(c).

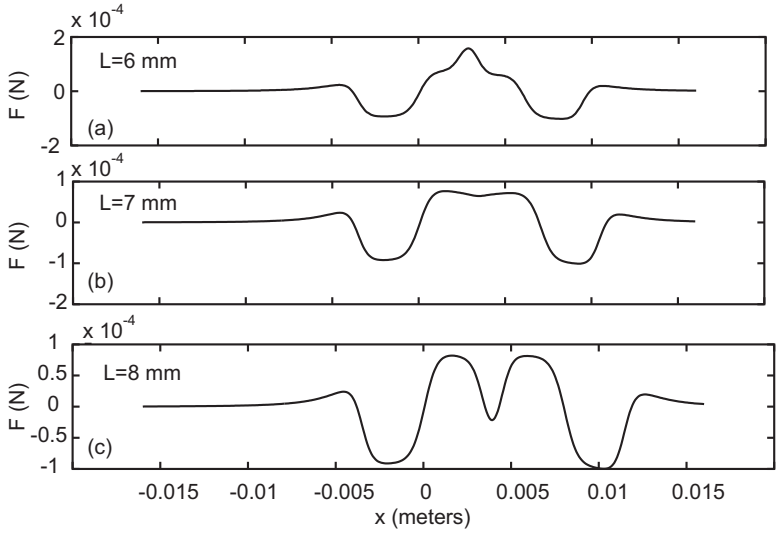

Figure 7. Simulation results showing the effect of distance between two coil centers on the force acting on a ferrofluid droplet at $y = 0$ mm, $z = 1$ mm, and $H_0 = 500$ A/m. The diameter of droplet is 1 mm. In the last case that L=8 mm, actuation in the full range is not possible, because the force has changed its sign between coil centers.

3.2. Motion of a ferrofluid droplet immersed in silicon oil

The forces acting on the droplet were described in the previous section. The force balance results in:

$$\begin{aligned} &F_{x_{\text{magnetic}}} - F_{x_{\text{drag}}} = m\frac{\mathrm{d}U}{\mathrm{d}t} \\ &\frac{V\Delta\chi}{\mu_0}\left(B_x\frac{\partial}{\partial x}B_x + B_y\frac{\partial}{\partial x}B_y + B_z\frac{\partial}{\partial x}B_z\right) - 3\pi D\eta \mathrm{U}\frac{1-2\eta/3\eta_{ff}}{1+\eta/\eta_{ff}} - m\frac{\mathrm{d}U}{\mathrm{d}t} = 0 \end{aligned} \tag{10}$$

where B_x, B_y, B_z are the components of the magnetic field induced by the coils and the permanent magnets, m is the mass and U is velocity of the ferrofluid droplet. The above equation can be solved numerically by Runge-Kutta method using the known force distribution. Although it is possible to use an analytical formula for the force distribution, the formulation is complex due to the summation of the coil segments and requires long computational time. For the convenience of the numerical solver, a polynomial function was fit to the force distribution using Matlab's curve fitting toolbox. The final force balance equation has then the form:

$$\frac{6}{\rho\pi D^3}\left(p_1x^6 + p_2x^5 + p_3x^4 + p_4x^3 + p_5x^2 + p_6x + p_7\right) - \frac{18\eta}{\rho D^2}\frac{\mathrm{d}x}{\mathrm{d}t} - \frac{\mathrm{d}^2x}{\mathrm{d}t^2} = 0 \tag{11}$$

where p_1 to p_7 are the constants determined by curve fitting algorithm for the polynomial function in use.

4. Results and discussion

The fabrication of the device and the experimental setup were reported in our previous paper [17]. The two coils on the top are connected to a constant current. The direction

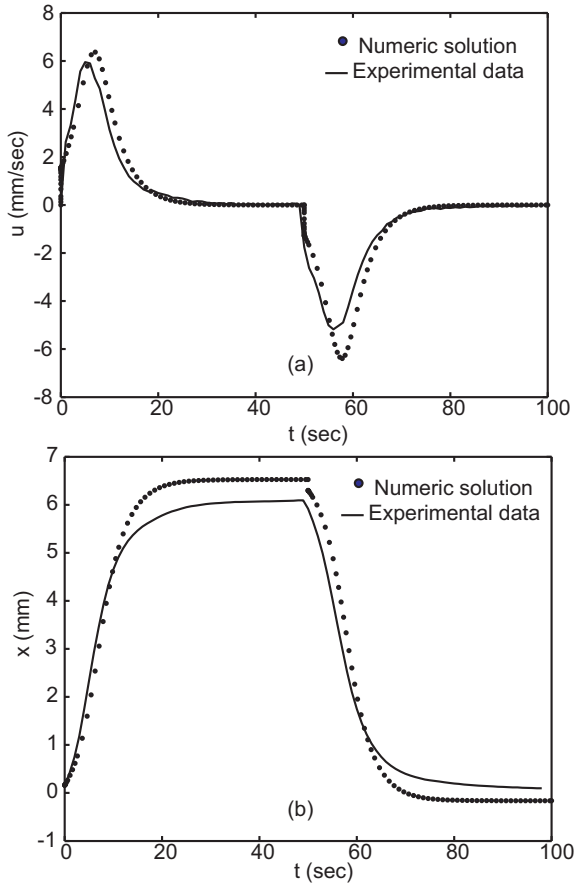

Figure 8. Comparison of experimental and numerical results ($H_0 = 500$ A/m, $I = 0.88$ A, $z = 5.5$ mm, $\nu = 100$ cSt, $d = 2.4$ mm): (a) velocity; (b) displacement.

of the current driving the two coils on the bottom are switched periodically. A miniature electromagnetic relay (Fujitsu, Takamisawa RY5WK) was used as the switching device. A single trigger signal was used for both the switching device and the CCD camera. Thus, the CCD camera is synchronized with the driving magnetic field. Accurate time measurement is achieved by fixing the frame rate of the CCD camera. The position of the ferrofluid droplet is extracted from the recorded images using Matlab. First, the gray scale image is converted into a binary image to identify droplet region. The centroid of the droplet is calculated and the position of the droplet is determined by tracking its centroid.

Figure 8 compares the numerical solution with experimental data. In the beginning of the motion, the droplet accelerated because the magnetic force increases as the droplet moves toward the next coil. After reaching its maximum velocity, the droplet decelerates and stops at the field maximum at the center of the next coil. The motion of the ferrofluid is mainly affected by the magnetic force and viscous drag force. The magnetic force depends on the parameters on the coils. A larger number of loops, higher driving current and a smaller gap between the loops increase the force of the coil [21]. Figure 9(a) shows that the magnetic force is proportional to the current. A large droplet

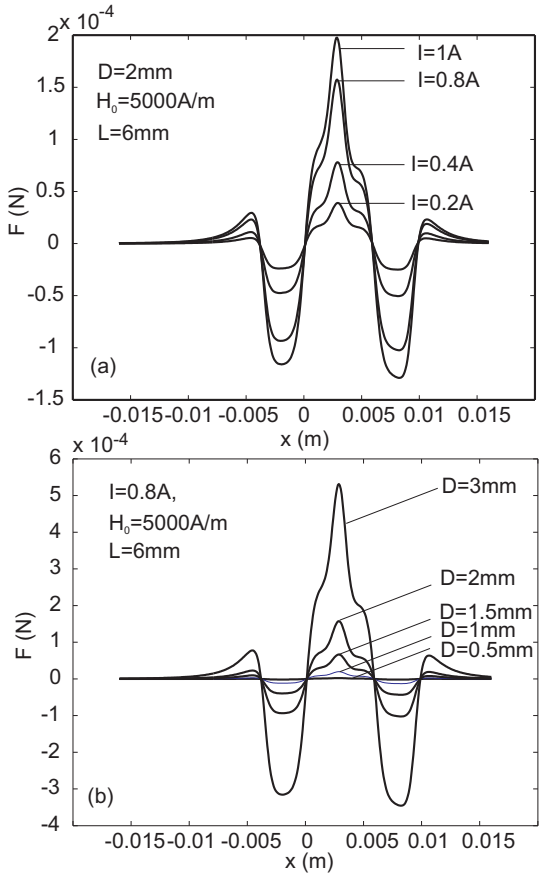

Figure 9. Magnetic force distribution at $y = 0$ mm, $z = 1$ mm: (a) Different actuating currents; (b) Different droplet diameters.

diameter also leads to a larger magnetic force, Figure 9(b). Since the magnetic force is proportional to the volume of the droplet, it increases with a power of three of the increase in droplet diameter.

Drag force depends on the size of the droplet and the viscosity of the carrier fluid. Figure 10 shows the effect of different parameters on the kinematics of the droplet motion immersed in silicon oil. The experimental data were taken from our work reported previously in [17]. Figure 10(a) shows both experimental and numerical results of droplet velocity for different diameters at an oil viscosity of $\nu = 100$ cSt and driving current of $I = 0.75$ A. Both experimental and numerical results show that the larger the droplet diameter, the higher is its velocity. As discussed above, the magnetic force on the droplet depends on the diameter with the power of three, while the drag force depends on the droplet diameter with the power of two. The increase in magnetic force due to the increase in droplet size dominates over the increase in drag force. Thus, at the same driving conditions a larger droplet has a higher velocity. Figure 10(b) shows that a higher driving current increases the velocity of the droplet and shortens its time to reach the maximum velocity. Figure 10(c) illustrates the effect of the viscosity of the carrier fluid on the motion of the ferrofluid droplet. At the same actuating condition

and droplet size the higher the viscosity, the lower is the velocity. The drag force is directly proportional to the viscosity of the carrier fluid. A higher viscosity increases the drag force and decreases the droplet velocity.

Figure 10 shows that numerical results agree relatively well with experimental data. The discrepancies between theory and experiments can have different reasons. Firstly, the droplet deforms when it moves [17]. Our model assumes a spherical shape for the droplet. Secondly, the microcoils on the PCB generate heat when the current is switched on. Although the silicone oil helps to spread the heat, a temperature distribution in the reservoir may lead to thermocapillary effect and affect the motion of the droplet. Moreover, the elevated temperature caused by Joule's heating of the coil changes the viscosity of the carrier fluid and affects the drag force. A further reason is the discrepancy between the simulated magnetic field and the actual magnetic field. As Figure 3 shows, the developed analytical results is slightly different from the experimental values. Since the recorded images only give us the spacial position in xy-plane, the exact z position of the droplet can not be measured. Although the force component F_z is small, it can elevate the ferrofluid droplet from the Teflon surface. The estimated position of $z = 5.5$ mm were therefore taken for all numerical results presented in Figures 8 and 10.

5. Conclusion

We reported a model of an one-dimensional actuation system for a ferrofluid droplet using planar microcoils. Based on the model of a single planar microcoil, the model for a pair of planar coils was developed and the actuation mechanism for a ferrofluid droplet was described. The forces acting on a ferrofluid droplet immersed in oil were calculated and subsequently used in the kinematic model describing the droplet motion. The modeling results agree relatively well with the experimental data. The discrepancies between the model and experimental data may be caused by the deformation of the droplet and the heat generated in the coils. The actuation concept reported in this paper can be used in a more complex droplet-based system for lab-on-a-chip applications.

Acknowledgement

The authors would like to thank the Agency of Science, Technology and Research, Singapore (A*Star, SERC Grant No. 0521010108) for their financial support.

References

[1] Teh SY, Lin R, Hung LH and Lee AP 2008 Droplet microfluidics *Lab on a Chip* **8** 198–220
[2] Song H, Chen DL, and Ismagilov RF 2006 Reactions in Droplets in Microfluidic Channels *Angewandte Chemie (International Edition)* **45** 7336
[3] Gijs MAM 2004 Magnetic bead handling on-chip: new opportunities for analytical applications *Microfluid nanofluid* 22–40
[4] Velev OD and Bhatt KH 2006 On-chip micromanipulation and assembly of colloidal particles by electric fields *Soft Matter* **2** 738–750

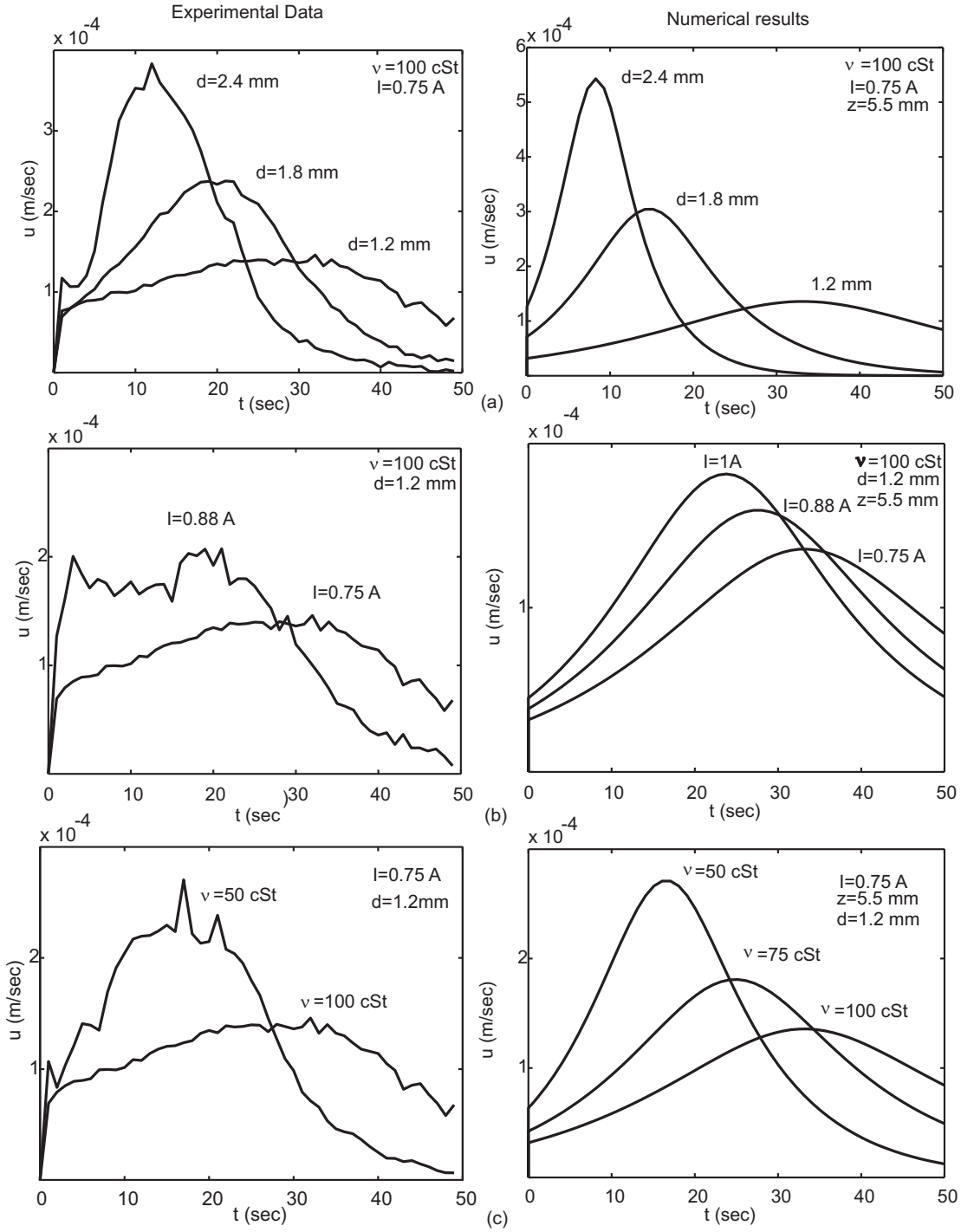

Figure 10. The effect of different parameters on the kinematics of ferrofluid motion immersed in silicon oil ($H_0 = 500$ A/m, $z = 5.5$ mm for numerical data). (a) Diameter of the droplet is changed and viscosity and current are fixed. (b) Current is changed and diameter of the droplet and viscosity are fixed. (c) The viscosity is changed and the current and diameter of the droplet are fixed.

[5] Pollack MG, Fair RB and Shenderov AD 2000 Electrowetting-based actuation of liquid droplets for microfluidic applications *Applied Physics Letters* **77** 1725

[6] Ting TH, Yap YF, Nguyen NT, Wong TN, Chai JCK and Yobas L 2006 Thermally mediated breakup of drops in microchannels *Applied Physics Letters* **89** 234101

[7] Wixforth A, Advalytix AG and Brunnthal G 2005 Flat fluidics: acoustically driven planar microfluidic devices for biological and chemical applications *Digest of Technical Papers - International Conference on Solid State Sensors and Actuators and Microsystems, TRANSDUCERS '05 1, art. no. 1D4.1* 143–146.

[8] Pamme N 2006 Magnetism and microfluidics *Lab on a Chip* **6** 24–38

[9] Ahn CH, Allen MG, Trimmer W, Jun YN and Erramilli S 1996 A fully integrated micromachined magnetic particle separator *Journal of Microelectromechanical Systems* **5** 151–158

[10] Ramadan Q, Samper V, Poenar D and Yu C 2005 Evaluation of Current-Carrying Wires for Manipulation of Magnetic Micro/Nanoparticles for Biomedical Applications International Journal of Nanoscience 4 **4** 489–499

[11] Lee CS, Lee H, Westervelt RM 2001 Microelectromagnets for the control of magnetic nanoparticles *Applied Physics Letters* **79** 3308–3310

[12] Rida A, Fernandez V and Gijs MAM 2003 Long-range transport of magnetic microbeads using simple planar coils placed in a uniform magnetostatic field *Applied Physics Letters* **83** 2396–2398

[13] Lehmann U, Hadjidj S, Parashar VK, Vandevyver C, Rida A and Gijs MAM 2006 Two-dimensional magnetic manipulation of microdroplets on a chip as a platform for bioanalytical applications *Sensors & Actuators: B. Chemical* **117** 457–463

[14] Lee H, Liu Y, Ham D and Westervelt RM 2007 Integrated cell manipulation system-CMOS/microfluidic hybrid *Lab on a Chip* **7** 331–337

[15] Nguyen NT, Ng KM and Huang XY 2006 Manipulation of ferrofluid droplets using planar coils *Applied Physics Letters* **89** 052509

[16] Guo ZG, Zhou F, Hao JC, Liang YM, Liu WM and Huck WTS 2006 Stick and slide ferrofluidic droplets on superhydrophobic surfaces *Applied Physics Letters* **89** 081911

[17] Nguyen NT , Beyzavi A , Ng KM , Huang XY 2006 Kinematics and deformation of ferrofluid droplets under magnetic actuation *Microfluid nanofluid* **5** 571–579

[18] Sun Y, Kwok YC and Nguyen NT 2007 A circular ferrofluid driven microchip for rapid polymerase chain reaction *Lab on a Chip* **7** 1012–1017

[19] Simon, MD and Geim, AK 2000 Diamagnetic levitation: flying frogs and floating magnets *Journal of Applied Physics* **87** 6200–6204

[20] Garcıa A, Carrasco JA, Soto JF, Maganto F and Morón C 2001 method for calculating the magnetic field produced by a coil of any shape *Sensors & Actuators: A. Physical* **91** 230–232

[21] Beyzavi A and Nguyen NT 2007 Modeling and optimization of planar microcoils *J. Micromech. Microeng* **18** 095018

[22] White 1974 *Viscous fluid flow* McGraw-Hill New York